Lateral sediment sources and knickzones as controls on spatio-temporal variations of sediment transport in an Alpine river

Cite As: Bekaddour, T, Schlunegger, F, Attal, M, Norton, KP & Föllmi, K (ed.) 2013, 'Lateral sediment sources and knickzones as controls on spatio-temporal variations of sediment transport in an Alpine river' *Sedimentology*, vol 60, no. 1, pp. 342-357.

DOI: 10.1111/sed.12009

Lateral sediment sources and knickzones as control on spatio-temporal variations of sediment transport in an Alpine River

Toufik Bekaddour[a], Fritz Schlunegger[a], Mikaël Attal[b] and Kevin P. Norton[c]

[a] Institut of Geological sciences, Baltzerstrasse, 1+3, 3012 Bern, Switzerland.

(E-mail: toufik.bekaddour@geo.unibe.ch)

[b] School of Geosciences, Institute of Geography, Drummond Street, Edinburgh, Uk.

[c] School of Geography, Environment and Earth Sciences, Victoria University of Wellington, New Zealand.

ABSTRACT

Modern mixed alluvial-bedrock channels in mountainous areas provide natural laboratories for understanding the time scales at which coarse-grained material has been entrained and transported from their sources to the adjacent sedimentary sink, where these deposits are preserved as conglomerates. This article assesses the shear stress conditions needed for the entrainment of the coarse bed particles in the Glogn River that drains the 400 km^2 Val Lumnezia basin, eastern Swiss Alps. In addition, quantitative data are presented on sediment transport patterns in this stream. The longitudinal stream profile of this river is characterized by three *ca* 500 m long knickzones where channel gradients range from 0.02 to 0.2 m/m, and where the active stream channel is confined into a <2 m wide gorge. Downstream of these knickzones, the stream is flat with gradients <0.01 m/m and widths ≥30 m. Measurements of the grain-size distribution along the trunk stream yield a mean *D84* value of *ca* 270 mm, whereas the mean *D50* is *ca* 100 mm. The consequences of the channel morphology and the grain size distribution for the time scales of sediment transport were explored by using a one-dimensional step-backwater hydraulic model (Hydrologic Engineering Centre – River Analysis System). The results reveal that along the entire trunk stream, a two to 10 year return period flood event is capable of mobilizing both the *D50* and *D84* fractions where the Shields stress exceeds the critical Shields stress for the initiation of particle motion. These return periods, however, varied substantially depending on the channel geometry and the pebble/boulder size distribution of the supplied material. Accordingly, the stream exhibits a highly dynamic boulder cover behaviour. It is likely that these time scales might also have been at work when coarse-grained conglomerates were constructed in the geological past.

Keywords Sediment transport, Critical shear stress, Return period floods, Particle entrainment, Basin hydrology, Swiss Alps

INTRODUCTION

Much research has been conducted with the aim of understanding the sedimentary architecture of streams that produce conglomerates either in basins or in valleys where these deposits are preserved as cut and fill systems (Miall, 1988). However, less work has been undertaken to examine how the pattern of sediment supply, paired with selective entrainment and deposition modifies the pattern of grain size and time scales of bedload transport. While the lack of subsidence in intra-mountain settings reduces the likelihood of preservation, such sedimentary records are often found as valley fill in glacially overdeepened basins and as terrace remnants. Here, coarse-grained channel bar deposits in the Glogn River, a tributary torrent of the Rhine River in the eastern Alps of Switzerland, have been used to explore the time scales at which bedload material has been transiting through this stream. Although coarse-grained deposits constitute up to 25% of the stratigraphies of proximal sedimentary basins (e.g. Allen et al., 2012) and of cut and fill systems in mountain valleys (e.g. Steffen et al., 2009), there are only a handful of studies that have addressed the mechanisms, and particularly the time scales at which coarse-grained bedload material has been transferred from their source in the mountain belts to the corresponding sedimentary basins (Whittaker, 1987; Allen, 1997; Jansen, 2006; Van den Berg and Schlunegger, 2012). In fluvial torrents and at the apexes of alluvial fans, the grain-size distribution of channel bars bears critical information about the boundary (or bed) shear stress conditions for the transport of material and, thus, about the magnitudes and variabilities of runoff. Previous analyses of these relations have converged on the notion that these hydrological variables have a measurable impact on the effective time scale of sediment transport and on the rate of fluvial incision into bedrock (e.g. Stock and Montgomery, 1999; Whipple and Tucker 1999; Whipple et al., 2000a; 2000b; Sklar and Dietrich, 2001; Molnar, 2001; Dadson et al., 2003; Whipple, 2004).

In mountainous areas, bedrock channel reaches and alluvial segments are both characteristic elements of a dynamic stream. These features are considered to be threshold-dominated as erosion and sediment transport only occur when the shear stress exerted by the flow on the river bed exceeds a critical value (Horton 1945; Montgomery and Dietrich, 1989). Furthermore, fluvial incision into bedrock and thus valley floor lowering require flood magnitudes that are large enough to mobilize the sediment cover in the channel, and that exceed the threshold to detach fragments from the bed and thus erode the substrate (Turowski et al., 2007, 2009; DiBiase and Whipple, 2011, Sklar and Dietrich, 2001). Because these systems are typically characterized by high thresholds for erosion and sediment transport, incision in these settings will be episodic and limited to the infrequent high magnitude floods (Tinkler, 1971).

This article investigates the time scales of sediment entrainment and, in particular, explores the thresholds to initiate motion of the coarse-grained sediment cover in the Glogn River that is the trunk stream of the *ca* 400 km^2 Val Lumnezia drainage basin, Eastern Swiss Alps (Graubünden) (Figure 1). Data are presented about the sedimentological fabric and particle-size distribution of longitudinal bars in the trunk stream, together with data about the morphometry and hydrology of the stream. These datasets were combined through the application of a coupled hydrological-sediment transport model in an effort to estimate the time scale of sediment transport in the trunk channel. Likewise, data were combined about hillslope-derived sediment flux in order to identify how the supply of large volumes of material has influenced these time scales. The ultimate scope is to estimate the minimum return period of floods that yield substantial modifications of the channel bars, which cause substantial sediment transport from upland to lowland areas, and which result in the lowering of the valley floor through erosion into bedrock.

STUDY AREA

Bedrock geology and valley morphology

The study area is located in the Central Alps of Switzerland (Figure 1A and B) that formed in response to the collision between the continental African and European plates at the end of the Mesozoic and during most of the Cenozoic. The bedrock of the study area is made up of a succession of Mesozoic meta-sedimentary rocks, which are referred to as 'Bündnerschiefer' in the regional literature (Figure 1B). These units have been assigned to the Ultrahelvetic and Penninic palaeogeographic domains on the western and the eastern side, respectively. In the Glogn River basin, the western valley flank comprises a >100 m thick Triassic succession of clays, evaporites and carbonates that is overlain by a Jurassic suite of schistose and quartz-rich calcareous sandstones. On the eastern side, the bedrock is a Jurassic to Cretaceous succession of sandy marbles, phyllites and green schists. Triassic limestones and dolostones of Penninic origins can be found as tectonic slivers in places. The valley floor follows the thrust plane that separates the Ultrahelvetic from the Penninic units. The bedrock on both valley flanks is partially covered by unconsolidated Quaternary glacial deposits.

The structural configuration (Figure 1C) has direct consequences for the valley morphology, as discussed by Schneider et al. (2008). On the western valley side, the bedrock dips parallel to the surface topography at angles between 15° and 35° (dip-slope situation), whereas the geological units dip into the slope on the eastern valley side (non dip-slope situation) (Figures 1D and E). Schneider et al. (2008) and Schwab et al. (2009) showed that this tectonic configuration has exerted a primary control on the hillslope sediment transport mechanisms in the entire catchment. On the western side, the dip-slope situation has promoted landsliding (for example, the Lumnezia landslide) with slip rates up to 10 cm per year, as revealed by geodetic surveys (e.g. Noverras et al., 1998). The continuous slip of

these landsides has transferred between 16,000 and 160,000 m^3 of material per year to the Glogn trunk stream and has impeded the establishment of a stable channel network, as discussed by Schneider et al. (2008) and Schlunegger et al. (2012). In contrast, on the eastern valley side, the orthogonal orientation of the topographic slope with respect to the bedding of the bedrock has caused the tributary streams to erode into the bedrock up to 150 m deep, with the result that the underlying lithology is exposed on the channel floor in nearly all tributary streams. In the Riein catchment that is the northernmost tributary basin on the eastern valley side (Figure 1B), bedrock avalanches have resulted in the transfer of >20,000 m^3 of coarse-grained material to the Glogn trunk stream during the past decades (Schwab et al., 2009).

Channel morphology, climate and runoff

The headwater reaches of the Rhein River have been the subject of sediment transport-related research since the classic study by Sternberg (1875). Here, the main focus is on the Glogn River, which originates at *ca* 3000 m above sea-level (m a.s.l.) in the Alps of Eastern Switzerland. Near Ilanz, it debouches into the Rhein River at an elevation of *ca* 700 m a.s.l. *ca* 30 km further downstream (Figure 2A and B). The longitudinal stream profile is characterized by three knickzones, as revealed by stream gradient data (Figure 2B and C). The upper two knickzones are *ca* 500 m long and have channel gradients that range from 0.02 to 0.2 m/m; they are genetically tied to the deep-seated Lumnezia landslide on the western valley side as inferred from a comparative analysis of 1956 and 2003 orthophotographs by Schwab et al. (2009). In particular, these authors revealed that slip of this landslide has shifted the Glogn River towards the opposite valley flank, and has promoted the development of the knickzones (e.g. Korup, 2006). Upstream and downstream of these knickzones, the stream is flat with gradients <0.01 m/m (Figure 2). In the

knickzones, the channel narrows to <2 m and exposes bedrock both on the channel floor and the bordering hillslopes. In these gorges, the bedrock exclusively comprises several tens of metres-thick suites of quartzite beds. In the flat reaches upstream and downstream of these knickzones, the stream has a cross-sectional width ≥30 m. It exhibits longitudinal gravel and coarser grained bars several tens of metres long and up to 5 m thick. Quartzite-rich bedrock knobs are exposed in places. Along the entire flat reaches, the bedrock comprises a suite of interbedded schists and decimetre-thick meta-sandstones. The third *ca* 100 m long knickzone is present where the Riein trunk stream debouches into the Glogn River (Figures 1B and 2). There, the channel hosts side bars several tens of metres long and the bedrock is exposed in a patchy pattern. The stream is nearly 40 m wide in this third knickzone and has a gradient that ranges between 0.05 and 0.1.

The climatic conditions in the study area are typical for a central Alpine basin, where runoff is dominated by snowmelt in spring and thunderstorms in summer. The daily mean water discharge in the Glogn River is *ca* 10 m^3/s, and the annual mean peak is *ca* 40 m^3/s; these are typically reached under low flow conditions (Federal Office for the Environment 2011 statistics). The mean annual precipitation in the Val Lumnezia is between 900 mm and 1350 mm, which is low compared with the average value in the Swiss Alps where mean precipitation rates are up to 2000 mm per year (e.g. Frei and Schär, 1998).

METHODS

The flood magnitude-frequency required to mobilise the sediments on the longitudinal bars was determined by using a combination of datasets including: (i) information about the channel morphology that is based on detailed mapping, field measurements and observations; (ii) grain size distributions measured along the Glogn trunk channel and in the tributary streams on both the eastern and western valley flanks; and (iii) calculations of the

shear stress required for the initiation of motion of coarse bed particles (Shields stress). The sediment sources were allocated and the channel morphologies measured based on detailed surveys in the field and on the 2 m light detection and ranging digital elevation model (LIDAR DEM). These data were complemented by information about the underlying bedrock in the entire drainage basin extracted from published maps. Grain-size data were measured in the field, in order to assess the critical Shields stresses required for entrainment of the coarse bed particles. Here, calculations were performed combining standard equations developed by Shields (1936) and original bedload equations developed by Meyer-Peter and Müller (1948) in an effort to relate grain size, bed shear stress and bedload transport capacity. Finally, the flood events and related shear stresses were simulated and calculated using a 1-D step-backwater hydraulic model [Hydrologic Engineering Centre – River Analysis System (HEC-RAS)].

Measurement of grain-size particle distributions

The surface grain-size distributions were measured along the trunk channel and tributaries by using the grid by number count method (Wolman, 1954). Figure 2A illustrates the samples sites and Figure 3 shows examples of bars in the Glogn River where grain-size populations were measured. A sampling grid of 4 m^2 was applied and 121 intercepts were counted. Wolman (1954) found that a count of 100 specimens provides consistent median values and reliable estimate of percentiles for the grain size-distribution patterns. This method was confirmed by experiments where one or multiple operators performed several counts (Wolman, 1954). Other studies have pointed out that 70 (Tinsdale, 1985) or even 60 specimen measurements were sufficient (Brush, 1961). In the trunk stream, grain-size data were collected from longitudinal bars with evidence for imbrication that indicates transport by fluvial traction (Miall, 1988a, b; Figure 3). Gravel and coarser-grained bars were

preferentially selected with sufficient distance (several metres) from the sides of the channel in order to avoid effects related to the potential supply of hillslope-derived material. The grid was spread out on each site and the grain measurements were taken under each intercept (grid by number counts). The measurements were carried out by two operators three times at each site. Following Rice and Church (1996), values of *D50* and *D84* (median grain size and 84th percentile of the distribution, respectively) were estimated from the combined set of measurements at each location (i.e. 363 measurements). The maximum estimated error was about 10%. For further explanation of the uncertainty assessment, the reader is referred to Van den Berg and Schlunegger (2012). Each specimen was picked and the intermediate *b* axis perpendicular to the long axis was measured at the widest point of the stone, as this is the dimension that would limit the sieve size through which it could pass (Kondolf et al., 2003; Attal and Lavé, 2006). This method was selected because it has been shown to provide an accurate estimation of the grain-size distribution patterns for mountainous streams (Kondolf and Li, 1992; Lenzi et al., 2006). These data were then used for *D84* incipient motion calculations. The *D84* was extracted from the dataset as this parameter characterizes the bed structure of the stream and tends to control its roughness (Howard, 1980; Prestegaard, 1983; Hey and Thorne, 1986; Howard, 1987; Grant et al., 1990; Jansen, 2006). Accordingly, a flood that exceeds the critical Shields stress for incipient motion of a grain of size *D84* is considered to substantially modify the channel morphology (Lenzi et al., 2006). Similarly, the *D50* fractions were used to quantify the sediment transport capacity.

Peak-discharge power law relations

The studied catchment is well-gauged and benefits from four gauging station records located at Glogn-Castrish (GC), Glogn-Peiden-Bad (GPB), Valser Rhein-Vals Platz (VRVP) and Peilerbach-Vals (PV; Figure 2). Each of the gauging stations has provided a continuous

record for at least 21 years. The records from these stations were provided by the Federal Office for the Environment (FOEN). These data were used to determine the power-law relationship between drainage area *A* and the modelled peak discharge Q_T for a given recurrence interval *T*:

$$Q_T = a_T A^{b_T} \quad (1)$$

where a_T and b_T denote *T*-dependent scaling factors and exponents. These values were determined through regression analysis of $\log(Q_T) - \log(A)$ plots, where $\log(a_T)$ and b_T are the regression intercept and the slope, respectively (Figure 4). The peak discharge magnitudes for floods exceeding the observation period of, for example, 21 years gauging record is determined by continuous probability distributions (gamma distribution; Swiss Federal Hydrological Service, 2002, 2005).

Bed particle entrainment

Shear stress at any point along the river conditions the erosion of its bed and banks, as illustrated by Wohl (1992, 1993), Turowski et al. (2007, 2009), Lenzi et al. (2006) and Yanites et al. (2010). Likewise, shear stress is important in controlling bedforms, the morphology of the channel and sediment transport rates (Bagnold, 1977, 1980; Knighton, 1999). Shear stress generally increases with increasing channel gradient and water depth, and the power to erode gravel and coarser-grained bars and banks will be larger with increasing flood magnitudes. Alternatively, shear stress decreases with increased channel widths. Reach-averaged shear stress is computed in the form (Shields, 1936):

$$\tau_b = \rho g R S \quad (2)$$

where τ_b is the shear stress applied by the flow, ρ is the fluid density (1000 kg/m^3), g is the gravitational constant, R is the hydraulic radius (m) and S is the channel gradient (m/m).

Shields (1936) defined a dimensionless parameter (Eq. 3) as the ratio of the fluid to the gravity forces applied to a single grain of interest (grain size D):

$$\tau^* = \frac{\tau_b}{\left[(\rho_s - \rho)gD\right]} \quad (3)$$

where τ^* is the Shields stress, ρ_s is the sediment density (2700 kg/m^3) and D is the grain size of interest. When the stress applied by the flow overcomes the gravity forces, incipient motion occurs: the dimensionless shear stress τ^* has reached the critical value τ_c^* (referred to as critical Shields stress).

Both the *D50* and the *D84* were considered as reference grain sizes D for sediment entrainment. For the entrainment of particles of size *D50*, the critical Shields stress value τ^*_{cD50} = 0.045 was used, which is commonly applied in studies of sediment transport (e.g. Buffington and Montgomery, 1997). For the entrainment of particles of size *D84*, however, we accounted for the fact that the mobility of clasts in a non-uniform mixture is largely controlled by the relative size of the material or the hiding/protrusion effect (Wilcock, 1997; Egiazaroff, 1965; Lenzi et al., 2006). It has been shown that sediment transport laws considering a large variety of grain sizes yield better results in mountain rivers (Wilcock, 1997, 2001). Among these, Egiazaroff, (1965) and Wilcock (1997, 2001) proposed a formula that considers hiding and protrusion effects by relating the critical shear stress at incipient motion τ_c^* to the ratio between the grain size of consideration (D_i) and a reference grain size (D_x):

$$\tau_c^* = a\left(\frac{D_i}{D_x}\right)^b \quad (4)$$

Here, $\tau^*_{cD84} = \tau_c^*$ was used, with (D_i) and (D_x) representing *D84* and *D50*, respectively. The exponent *b* varies between 0 (full size-selective entrainment; i.e. no hiding/protrusion effects) and -1 (complete equal mobility conditions; Parker et al., 1982; Komar and Li, 1986; Buffington and Montgomery, 1997; Church et al., 1998; Lenzi et al., 2006). Following Komar (1987), values of 0.045 and -0.6 were assigned to the coefficient *a* and the exponent *b*.

The critical Shields stress for the entrainment of a grain of size *D84* was then calculated considering the maximum (560 mm), minimum (100 mm) and mean values (270 mm) of *D84* for all sites using Eq. 4, yielding three different values (0.01, 0.02 and 0.04, respectively) where the critical Shields stress increases with decreasing grain of size *D84* and vice versa. Note that these inverse relations are related to the hiding/protrusion effects of poorly sorted material. For the sake of simplicity, the mean *D50* was kept at a fixed level for all sites during this calculation. Then the conditions were calculated for incipient motion of sediment along the Glogn River related to flood magnitudes with return periods of two, 10 and 100 years using Eqs 3 and 4 (Shields, 1936; Meyer-Peter and Müller, 1948).

Sediment transport

The sediment transport capacity computation was based on the original bedload equation developed by Meyer-Peter and Müller (1948):

$$(q_b)_* = 8\left[\tau^* - \tau_c^*\right]^{1.5} \quad (5)$$

where $(q_b)_*$ is the dimensionless transport rate:

$$(q_b)_* = \frac{q_b}{\left[\left(\frac{\rho_s - \rho}{\rho}\right) g D^3\right]^{0.5}} \quad (6)$$

Here, the grain size *D* corresponds to the *D50*. The volumetric bedload flux per unit width q_b is then used to compute the total transport capacity for each return period:

$$Q_b = q_b W \quad (7)$$

Here, *W* is the calculated channel width at each return period (i.e. recurrence intervals).

Hydraulic modelling

Analyses focused on whether Shields stresses generated by floods with recurrence intervals of two, five, 10, 30, 50 and 100 years were capable of exceeding the critical Shields stresses τ^*_{cD84} and τ^*_{cD50}. Only the two, 10 and 100 year floods are presented here since they are the most relevant return periods for the purpose of this study and because the differences between, for example, two and five year floods are negligible. Near the outlet of the basin (in close proximity to Ilanz), the calculated peaks of these return period floods (based on continuous probability distributions of gauging records, see above) are approximately equal to 100 m^3/s, 200 m^3/s and 300 m^3/s, respectively. The boundary (or bed) shear stress τ_{Q_T} was calculated with HEC-RAS (see next paragraph) for each flood magnitude-frequency, where R_{QT} is the flood specific hydraulic radius, *Q* is the discharge and *T* is the return period using the following relations:

$$\tau_{Q_T} = \rho g R_{Q_T} S \quad (8)$$

The Shields stress exerted on the river bed particles during a *T*-year flood, on both *D50* and *D84* is defined as follows (Shields, 1936):

$$\tau^*_{Q_T D_{50}} = \frac{\tau_{Q_T}}{(\rho_s - \rho) g D_{50}} \quad (9)$$

and:

$$\tau^*_{Q_T D_{84}} = \frac{\tau_{Q_T}}{(\rho_s - \rho) g D_{84}} \quad (10)$$

The Shields stress (Eqs 9 and 10) and the related total transport capacity (Eq. 7) were calculated using HEC-RAS (Hydrologic Engineering Center, 1998; 2008). This model was selected because it has been successfully applied in mountainous basins under similar conditions as those found in the study area (Miller and Cluer, 1998; Jansen, 2006; Kidson et al., 2006). The HEC-RAS model calculates a steady flow water surface profile that is computed from one cross-section to the next. This calculation is done by solving the one-dimensional energy equation with an iterative algorithm, where the total energy at any given location along the stream is the sum of the potential energies and the kinetic energy. The lateral and semi-lateral flows are not calculated directly by the model. Energy losses by friction are considered using Manning's equation, where Manning's *n* roughness coefficient is based on empirical relations between channel gradient, *S,* which is used as proxy for the friction slope, and the hydraulic radius, *R* (Jarrett, 1984):

$$n = 0.32 S^{0.38} R^{-0.16} \quad (11)$$

Values of Manning's n were approximated by running at least five simulations for each flood magnitude-frequency (i.e. two, five, 10, 30, 50 and 100-year floods). Finally, those Manning's

n values that were accepted as the best fit for each run were used (i.e. the values were stabilized and not liable to any variations). The *n* values predicted by Eq. (11) in the present study site range from 0.01 to 0.1 for all simulations, which is within the range of measured values determined by Jarrett (1984) for high-gradient rivers.

Finally, the HEC-RAS model requires hydraulic and detailed cross-sectional data of the stream bed. The channel cross-sections were extracted at 10 m intervals along the entire channel, using a standard GIS environment. The channel bed geometry data (i.e. x, y and z) were collected at *ca* 2600 sites within a GIS environment from a 2 m LiDAR DEM with a vertical accuracy of less than 0.5 m provided by the Swiss Federal Office of Topography (Swisstopo). The depth of the water column in the study stream channel doesn't exceed 100 mm during usual flow stage. Furthermore, the LiDAR DEM are usually made during periods of low flow stage which potentially make that LiDAR DEM is a reasonably good representation of the ground elevation for any detailed hydraulic and hydrological modelling..

RESULTS AND INTERPRETATION

Grain-size distribution and origin of material

The results of the grain-size measurements show strong variability of the *D84* and *D50* values along the entire trunk stream (Figure 5). The largest *D84* value of 560 mm was measured just upstream of the major knickzone, where landsliding has pushed the Glogn River towards the opposite valley flank during the past decades as revealed by comparative photogrammetry (Schwab et al., 2009). There, a measurement of 230 mm was recorded for the *D50*. At the downstream end of this knickzone, the grain-size values then decrease to 105 mm and 55 mm for *D84* and *D50*, respectively. A second site (S4; Figure 2A) with coarse material was identified 20 m after the confluence with the Valser Rhein, where a *D84*

of 175 mm was measured (50 mm for the *D50*). From there, the *D84* decreases to 130 mm (51 mm for the *D50*) and finally to 95 mm (50 mm for the *D50*) *ca* 4 kms after the confluence with the Valser Rhein. A third site with a large *D84* value of 285 mm (100 mm for the *D50*) is identified a few meters after the confluence with the Riein tributary torrent (S1; Figure 2A). Finally, large *D84* and *D50* values of 500 and 150 mm, respectively, were measured *ca* 1.5 km upstream of Ilanz where the Glogn River undercuts a landslide (S7; Figure 2A).

The *D84* (and *D50*) values in the tributary streams are between 420mm and 450 mm on the western valley flank (*D50* = 270 mm and 140 mm) and 440 mm (*D50* = 220 mm) in the Pitasch River that originates on the eastern valley side. The grain size in the Riein River has a *D84* value of 285 mm (*D50* = 100 mm), which is identical to the grain size of the material in the Glogn trunk stream immediately downstream of the confluence. Finally, the *D84* in the Val Uastg is 282 mm (130 mm for the *D50*).

The grain-size distribution patterns in the Glogn trunk stream appear to be controlled largely by the supply of the material from either the bordering hillslopes or from the tributary torrents, particularly on the eastern flank. On these valley sides, two potential sediment sources have to be considered which are either bedrock landslides/rock avalanches or unconsolidated glacial deposits. The deep-seated bedrock landslides/rock avalanches are favoured as the major contribution of material to the Glogn River. This interpretation was based on the field survey herein, the results of the grain-size analysis, and on photogrammetry-based assessments of sediment supply for the past decades. In particular, Schwab et al. (2009) identified three major sediment sources along the Glogn River. The first site of a major sediment supply is located near the upstream end of the uppermost knickzone where slip of the Lumnezia landslide has pushed the Glogn trunk stream towards the opposite valley flank. A second sediment source is located immediately downstream of the confluence with the Valser Rhein where landsliding on the western valley flank has shifted the Glogn trunk stream *ca* 20 m towards the opposite site during the past tens of

years. The Riein River was identified by Schwab et al. (2009) as a third site of a major sediment source where rock avalanches have resulted in the supply of 20,000 m^3 of material during the past decades. Finally, a landslide on the eastern valley side *ca* 1.5 km upstream of Ilanz is considered to have supplied sediment where the Glogn River has undercut the hillslope on the eastern side. These sediment sources are characterized by coarse-grained material, as revealed by the grain-size measurements in streams perched on the landslide and in the incised tributary streams. Accordingly, the large grain-size variability along the Glogn trunk stream was interpreted as a direct consequence of the non-uniform pattern of sediment supply by mass wasting (e.g. Rice and Church 1996; Korup 2006; Attal and Lave, 2006; Whittaker et al., 2010). In particular, sediment supply of the Riein River (through one or multiple rock avalanches in the headwater reach) appears to completely dominate the current grain-size distribution of the Glogn trunk stream for a limited distance as indicated by the identical *D84* values in the tributary channel and the trunk stream immediately after the confluence. However, *D84* and *D50* tend to decrease rapidly downstream of the sediment sources, suggesting that downstream fining also occurs (e.g. Paola and Seal, 1995). Accordingly, the large variability of grain size along the Glogn River reflects an imbalance between the spatio-temporal scales at which sediment has been supplied from lateral sources, and those of sediment transport and deposition in the trunk stream.

Hydraulic modelling

The modelled bed shear stresses for floods with return periods of two, 10 and 100 years are presented in Figure 6. Note that the pattern is identical for all flood magnitudes, with a systematic increase in shear stress with increasing flood magnitude and highest values along the major knickzones. Likewise, the shear stress curves mirror the channel gradient variation along the entire channel. Shear stress values of floods with two year return periods

are between 600 N/m^{2}and 1600 N/m^2 in the uppermost two knickzone reaches where bedrock is exposed on the channel floor. These values are substantially lower <200 N/m^2 in the flat segments. In the lowermost third knickzone, the bed shear stress varies between 250 N/m^2 and 350 N/m^2. Floods with 10 and 100 year return periods are characterized by a higher shear stress in the upper two knickzone reaches, where shear stress values range between 900 N/m^2 and 1700 N/m^2 and 1000 N/m^2 and 1900 N/m^2, respectively. In the lowermost third knickzone, shear stress values range between 300 N/m^2 and 600 N/m^2 for flood magnitudes with return periods of 10 years and 100 years, respectively. Likewise, the flat segments show values of shear stress between 300 N/m^2 and 400 N/m^2 for the same flood events.

The conditions for incipient motion of the *D50* and *D84* are shown in Figure 7A and B for flood magnitudes with return periods of two, 10 and 100 years, respectively. The two year flood is clearly exceeding the critical Shields stress in the steep segments. However, in the flat segments, the Shields stress applied on *D84* is not far from the critical Shields stress when assuming the minimum *D84* value for all sites, but it still remains above the critical Shields stress values when considering the maximum and mean *D84* values. These negative relations between the *D84* and the critical Shields stress are explained by hiding/protrusion effects, which are commonly found in poorly sorted gravel beds (see above and Eq. 4). Floods with return periods of 10 and 100 years largely exceed the critical Shields stress to entrain the *D84* along the entire stream. Two year and larger floods are capable of entraining the *D50* along the entire stream.

Because the *D84* represents the grain size that characterizes the bed structure of the stream (Howard, 1980; Jansen, 2006), the motion of these grains will result in a substantial modification of the riverbed architecture. Accordingly, in the knickzones, a change of the channel morphology was predicted on a yearly basis; this could either be accomplished through vertical incision into bedrock or lateral channel migration. Currently, there is a lack of

quantitative information to solve this question unequivocally. However, given the high erosional resistance of bedrock where quartzite beds are exposed, a tentative interpretation is that lateral migration of the trunk channel associated with bank collapse is the predominant channel forming process. Likewise, bed form changes on a yearly basis are also expected in the flat reaches. However, because the Shields stress is close to the critical value in the flat segments for two year floods, only small changes were anticipated.

The calculated sediment transport capacity values are illustrated on Figure 8. As for the bed shear stress, the transport capacity strongly depends on both channel geometry and the discharge magnitudes; they peak around the knickzones and are nearly constant along the flat segments.

DISCUSSION

Controls of channel geometry on sediment transport

The analysis here illustrates that the bed shear stress and the sediment transport capacity during flood of two, 10 and 100 year return periods are capable of mobilising the supplied material along the entire Glogn River, including the flattest segment along the lowermost reach. In the knickzones, the stream appears to be more efficient at transporting the supplied material as bedload at all return period floods. These circumstances illustrate the controls of channel gradients on the time scales of sediment transport and bed form changes. The results of this study thus support the idea that sediment transport in mountainous streams strongly depends on the stream geometry (e.g. Turowski et al., 2007, 2009). Similarly, sediment transport rates (which relate to the geomorphological work according to Wolman and Miller, 1960) and the capacity to reshape the landscape (which corresponds to the geomorphological effectiveness according to Wolman and Gerson, 1978)

also occur in response to yearly and decadal flood events in the knickzones and the lowermost flat reaches, respectively.

Controls of sediment supply on the channel network

The large variability of grain-size distribution along the trunk stream points towards an imbalance between the lateral supply of sediment from the valley sides, and the capacity of the stream to transport the delivered sediments along the entire channel. The complex and poorly sorted nature of the grain-size distribution was related to the large lateral sediment input in the form of landslides and rock avalanches. Poorly sorted bars are in close proximity to major lateral sediment sources. This observation is particularly true in the flat channel reach downstream of the confluence with the Riein torrent where this easterly tributary stream has supplied large volumes of sediment to the trunk stream, but where the transport capacity is generally low (see above, and Schwab et al., 2009). Likewise, the Lumnezia landslide and a landslide south of Ilanz on the western and eastern valley flanks, respectively, have been the source of large volumes of sediment supplied to the Glogn River. In contrast, channel reaches, which lack substantial lateral sediment input and mainly experience sediment transport from upstream, are characterized by better-sorted channel bars with down-stream fining trends (Rice and Church 1998; Rice 1999). Indeed, better-sorted channel bars and downstream fining trends are found, for instance, below the inferred supply of landslide-derived material (between the downstream distance of 8 km and 14 km on Figure 5B). The situation, however, is different in the two knickzones further upstream. There, the absence of a sediment cover suggests a high ability of the stream to entrain and transport sediment. These conditions are likely to promote changes of the channel morphology through lateral erosion or vertical incision since no significant sediment cover will protect the channel bed from erosion (e.g. Turowski et al., 2007, 2009).

Variations in time scales of sediment entrainment and erosional regime

The calculations presented here imply that large floods with a return period longer than *ca* 10 years are able to mobilise sediment along the entire length of the stream. Moderate floods on the other hand (for example, two -year floods) will fully entrain sediment only in the knickzones, whereas the shear stress will be close to the stress for incipient motion in the flat reaches. In these flat segments, it is hypothesized that such floods will selectively entrain the finer fraction of the sediment, leading to a progressive coarsening and armouring of the gravel/boulder bars, which may reduce further the mobility of the sediment. Supply and selective deposition of coarse sediment transferred from the knickzones upstream will also contribute to the coarsening of the sediment along the flat reaches (Paola and Seal, 1995; Attal and Lavé, 2006). These effects were interpreted to result in an overall high degree of clast interlocking in the flat reaches.

In relation to the fluvial erosional mechanisms, the present results show that the study basin is a mixed system where detachment-limited conditions prevail in steep reaches, whereas transport-limited conditions characterize the fluvial erosional dynamics in the flat channel segments (see also Sklar et Dietrich, 1998; Turowski et al., 2007, 2009). The consequences of these spatial variations in the river behaviour are two different scenarios of stream evolution in the sense that downcutting paired with lateral bank erosion (however limited by the nature of bedrock, see above), will prevail in the supply-limited steep reaches, whereas mainly lateral bank erosion is predicted to dominate in the flat transport-limited segments (Turowski et al., 2007; Yanites et al., 2010). It is anticipated that the processes responsible for the evolution of channel morphology in these segments with contrasting behaviour will operate at different time scales. Thus, the interpretation here is that bedrock (detachment-limited) channel reaches are partly decoupled from the flat alluvial (transport-limited)

segments in the sense that both may develop independently from each other over time scales that have yet to be quantified.

Implications for the construction of conglomerates

With respect to conglomerate formation, the process of selective deposition and gravel and coarser grained bar formation is dependent on the relative time scales of fluvial aggradation and effective floods. As shown by the simulations, decadal floods are capable of reworking the gravel reaches. If there has not been substantial deposition (requiring accommodation space), then the gravels will be purged and a new system of bars will form. Otherwise, the gravel bars remain as a sedimentary record (e.g. Miall, 1988a).

During the formative stages of mountain building, accommodation space is common in the form of foreland basins. In such systems, accumulation of gravels is often related to allocyclic mechanisms (e.g. Paola et al., 1992). It is unlikely that the Glogn can be considered as an analogue for such streams. However, the analysis herein suggests that during later stages of orogenic development, source areas may be the major controls on grain size in gravel stream deposits. Selective deposition results in the preservation of coarse sediment within the orogen. These records will therefore mainly be preserved in valley fills and terraces within the mountain valley and near the foothills.

CONCLUSION

This study demonstrates the merit of the critical Shields stress approach paired with basin hydraulic analyses for understanding the dynamics of the boulder bed cover, the bedrock erosional mechanisms and the evolution of channel morphology in a mountainous stream. Grain-size distribution measurements and field investigations reveal that stream gradients, flood magnitude-frequency and the spatio-temporal scales at which sediment is supplied

from both valley sides and tributary streams exert a major control on the sediment transport mechanisms along the Glogn River. It was found that along the knickzones of the Glogn trunk stream and along almost the entire channel, a flood event with a two year return period is capable of mobilising sediment on the channel bed as the Shields stress exceeds the critical Shields stress for incipient motion of bed particles. Sediment transport, however, is most effective in the steep knickzone reaches, where exposure of bedrock likewise indicates supply-limited conditions and thus efficient removal of sediment. However, along the flattest reaches near the downstream end of the river, the Shields stress applied on the channel bed during a two year return period appears to be slightly above but near the critical Shields stress values. It would be expected that in these flat reaches, the entrainment of *D84* will be limited during floods with a two year return period. As a consequence, the degree of interlocking of coarse-grained material increases, which ultimately leads to enhanced stabilization of the channel bed at these segments and, thus, to a higher threshold condition for bed material entrainment. However, decadal and larger floods are capable of moving both the *D50* and *D84* fractions along the entire stream including the flattest segments. This implies that discharge events of these magnitudes represent effective floods that result in the mobilisation of hillslope-derived material along the entire Glogn River. This article proposes that floods with these return periods might also have been at work for the construction of conglomerate beds preserved in many sedimentary records.

ACKNOWLEDGMENTS

This paper greatly benefitted from constructive discussions with Fabien Van den Berg. Dirk Rieke-Zapp was very helpful with the handling of the GIS environment. We are grateful to G. Simpson and B. McArdell for their careful review and the constructive comments, which greatly improved the manuscript. SwissTopo is acknowledged for providing the LIDAR DEM.

The Federal Office for the Environment (FOEN) allowed us to use the hydrological data. This paper was financed through SNF grants 200020-121680 and 20T021-120464, and ESF TopoEurope.

References

Allen, P.A. and Heller, P.L. (2012) Dispersal and preservation of tectonically generated alluvial gravels in sedimentary basins. In: Tectonic of Sedimentary Basins:

Recent Advances (Eds C. Busby, A. Azor, P.A. Allen and P.L. Heller), pp. 111–130. John Wiley-Blackwell & Sons, Ltd, Chichester, UK, doi:10.1002/9781444347166.ch6.

Attal, M. and Lav_e, J. (2006) Changes of bedload characteristics along the Marsyandi River (central Nepal), implications for understanding hillslope sediment supply, sediment load evolution along fluvial networks, and denudation in active orogenic belts. Geol. Soc. Am. Spec. Pap., 398, 143–171.

Bagnold, R.A. (1977) Bed load transport by natural rivers. Water Resour. Res., 13, 303–312.

Bagnold, R.A. (1980) An empirical correlation of bedload transport rates in flumes and natural rivers. Proc. Roy. Soc., 372A, 453–473.

Brush, L.M. (1961) Drainage basins, channels, and flow characteristics of selected streams in Central Pennsylvania. U.S. Geol. Surv. Prof. Pap., 282-F, 145–180.

Buffington, J.M. and Montgomery, D.R. (1999) Effects of hydraulic roughness on surface textures of gravel-bed rivers. Water Resour. Res., 35, 3507–3521.

Dadson, S.J., Hovius, N., Chen, H.G., Dade, W.B., Hsieh, M. L., Willett, S.D., Hu, J.C., Horng, M.J., Chen, M.C., Stark, C.P., Lague, D. and Lin, J.-C. (2003) Links between erosion, runoff variability and seismicity in the Taiwan orogeny. Nature, 426, 648–651.

DiBiase, R.A. and Whipple, K.X. (2011) The influence of erosion thresholds and runoff variability on the relationships among topography, climate, and erosion rate. J. Geophys. Res., 116, F04036.

Egiazaroff, I.V. (1965) Calculation of non-uniform sediment concentrations. J. Hydraul. Div., 91, 225–247.

Frei, C. and Schär, C. (1998) A precipitation climatology of the Alps from highresolution rain-gauge observations. Int. J. Climatol., 18, 873–900.

Grant, G.E., Swanson, F.J. and Wolman, M.G. (1990) Pattern and origine of steppend-bed morphology in high gradient, western cascades, Oregon. Bull. Geol. Soc. Am., 102, 340–352.

Horton, R.E. (1945) Erosional development of streams and their drainage basins: hydrophysical approach to quantitative morphology. Bull. Geol.Soc. Am.,, 56, 275–370.

Hey, R.D. and Thorne, C.R. (1986) Stable channels with mobile gravel beds. J. Hydraul. Eng., 112, 671–689.

Howard, A.D. (1980) Thresholds in river regimes. In: Thresholds in Geomorphology (Eds D.R. Coates and J.D.

Vitek), pp. 227–258. Allen and Unwin, Boston. Howard, A.D. (1987) Modelling fluvial systems: rock-, gravel-, and sand-bed channels. In: River Channels: Environment and Process (Ed. K.S. Richards), pp. 69–94. Blackwell, Oxford, UK.

Hydrologic Engineering Center (1998) HEC-RAS River Analysis System: Hydraulic Reference Manual. US Army Corps of Engineers, Davis, CA, 189 pp. Hydrologic Engineering Center (2008) Program. US Army Corps of Engineers, Davis, CA.

Komar, P.D. and Li, Z. (1986) Pivoting analyses of the selective entrainment of sediments by shape and size with application to gravel threshold.. Sedimentology, 3, 413–423.

Jansen, J.D. (2006) Flood magnitude-frequency and lithologic control on bedrock river incision in post-orogenic terrain. Geomorphology, 82, 39–57.

Jarrett, R.D. (1984) Hydraulics of high-gradient streams. J. Hydraul. Eng., 110, 1519–1539.

Kidson, R.L., Richards, K.S. and Carling, P.A. (2006) Hydraulic model calibration for extreme floods in bedrockconfined channels: case study from northern Thailand. Hydrol. Process., 20, 320–344.

Knighton, A.D. (1999) Downstream variation in stream power. Geomorphology, 29, 293–306.

Komar, P.D. (1987) Selective gravel entrainment and the empirical evaluation of flow competence. Sedimentology, 34, 1165–1176.

Kondolf, G.M. and Li, S. (1992) The pebble count technique for quatifying surface bed material in instream flow studies. Rivers, 3, 80–87.

Kondolf, G.M., Lisle, T.E. and Wolman, G.M. (2003) Bed sediment measurement. In: Tools in Fluvial Geomorphology (Eds G.M. Kondolf and H. Piegay), pp. 347 –395. John Wiley and Sons, Chichester, UK.

Korup, O. (2006) Rock-slope failure and the river long profile. Geology, 34, 45–48.

Lenzi, M.A., Luca Mao, L. and Comiti, F. (2006) When does bedload transport begin in steep boulder-bed streams? Hydrol. Process., 20, 3517–3533.

Meyer-Peter, E. and M€uller, R. (1948) Formulas for Bed-Load Transport. Proceedings of the Second Meeting of International Association of Hydraulic Engineering Research. Stockholm, Sweden, pp39–64.

Miall, A.D. (1988a) Facies architecture in clastic sedimentary basin. In: News Perspectives in Basin Analysis (Eds K. Kleinspehn and C. Paola), pp. 67–81. Springer, New York.

Miall, A.D. (1988b) Architectural elements and bounding surfaces in fluvial deposits: anatomy of the Kayenta Formation (Lower Jurassic), southwest Colorado. Sed. Geol., 55, 233–262Miller, A.J. and Cluer, B.L. (1998) Modeling considerations for simulation of flow in bedrock channels. Geophys. Monogr. Ser., 107, 61–104.

Molnar, P. and Ramirez, J.A. (2001) Recent trends in precipitation and streamflow in the Rio Puerco Basin. J. Climate, 14, 2317–2328.

Mosley, M.P. and Tinsdale, D.S. (1985) Sediment variability and bed material sampling in gravel bed rivers. Earth Surf. Proc. Land., 10, 465–482.

Noverraz, F., Bonnard, C., Dupraz, H. and Hugenin, L. (1998) Grands glissements de versants et climat. ETHZ, Zürich, 314 pp.

Paola, C. and Seal, R. (1995) Grain size patchiness as a cause of selective deposition and downstream finding. Water Resour. Res., 31, 1395–1407.

Paola, C., Heller, P.L. and Angevine, C.L. (1992) The largescale dynamics of grain-size variation in alluvial basins, 1: Theory. Basin Res., 4, 73–90.

Parker, G., Klingeman, P.C. and McLean, D. (1982a) Bedload and size distribution in paved rave-bed streams. J. Hydraul. Div., 108, 544–571.

Parker, G., Dhamotharan, S. and Stefan, H. (1982b) Model experiments on mobile, paved gravel bed streams. Water Resour. Res., 18, 544 571. Prestegaard, K.L. (1983) Bar resistance in gravel bed streams at bankfull stage. Water Resour. Res., 19, 472–476.

Rice, S.P. (1999) The nature and controls on downstream fining within sedimentary links. J. Sed. Res., 69, 32–39.

Rice, S.P. and Church, M. (1996a) Bed material texture in low-order streams on the Queen Charlotte Islands, British Columbia. Earth Surf. Proc. Land., 21, 1–18.

Rice, S.P. and Church, M. (1996b) Sampling surficial fluvial gravels: the precision of size distribution percentile estimates. J. Sed. Res., 66 3, 654–665.

Rice, S.P. and Church, M. (1998) Grain size along two gravel bed rivers: statistical variation, spatial pattern and sedimentary links. Earth Surf. Proc. Land., 23, 345 363.

Schneider, H., Schwab, M. and Schlunegger, F. (2008) Channelized and hillslope sediment transport and the geomorphology of mountain belts. Int. J. Earth Sci., 97,179–192.

Schwab, M., Schlunegger, F., Schneider, H., St€ockli, G. and Rieke-Zapp, D. (2009) Contrasting sediment flux in Val Lumnezia (Graub€unden, Eastern Swiss Alps), and implications for landscape development. Swiss J. Geosci., 102, 211–222.

Shields, A. (1936) Application of Similarity Principles and Turbulence Research to Bedload Movement (English Translation), Vol. 102. Hydrodynamics Laboratory, California Institute of Technology, Publication, Pasadena, CA, 36 pp.

Sklar, L. and Dietrich, W.E. (1998) River longitudinal profiles and bedrock incision models: stream power and the influence of sediment supply. In: Rivers Over Rock:

Fluvial Processes in Bedrock Channels (Eds J.K. Tinkler and E.E. Wohl), Geophys. Monogr. Ser., 107,237–260. AGU, Washington, DC.

Steffen, D., Schlunegger, F. and Preusser, F. (2009) Drainage basin response to climate change in the Pisco valley. Peru Geol., 37, 491–494.

Sternberg, H. (1875) Undersuchungen €uber L€angen- und Querprofile geschiebef€uhrender Fl€usse. Z. Bauwesen, 25, 483–506.

Swiss Federal Hydrological Service (2005) Hydrologisches Jahrbuch der Schweiz, Bundesamt fu¨ r Umwelt. Wald und Landschft, Bern, 531.

Tinkler, K.J. (1971) Active valley meanders in south-central Texas, their wider implications. Geol. Soc. Am. Bull, 82, 1783–1800.

Turowski, J.M. and Richenmann, D. (2009) Tools and cover effects in bedload transport observation in the Pitzbach. Austria. Earth Surf. Proc. Land., 34, 26–37.

Turowski, J.M., Lague, D. and Hovius, N. (2007) Cover effect in bedrock abrasion: implication for fluvial modelling and river morphology. J. Geophys. Res., 11, 2.

Van den Berg, F. and Schlunegger, F. (2012) Alluvial cover dynamics in response to floods of various magnitudes: the effect of the release of glaciogenic material in a Swiss Alpine catchment. Geomorphology, 141–142, 121–133.

Whipple, K.X. (2004) Bedrock rivers and the geomorphology of active orogens. Annu. Rev. Earth Planet. Sci., 32, 151–185.

Whipple, K.X. and Tucker, G.E. (1999) Dynamics of the stream power river incision model: implications for height limits of mountain ranges, landscape response timescales and research needs. J. Geophys. Res., 104, 17661–17674.

Whipple, K.X., Hancock, G.S. and Anderson, R.S. (2000a) River incision into bedrock: mechanics and relative efficacy of plucking, abrasion, and cavitation. Bull. Geol. Soc. Am., 112, 490–503.

Whipple, K.X., Snyder, N.P. and Dollenmayer, K. (2000b) Rates and processes of bedrock incision by the Upper Ukak River since the 1912 Novarupta Ash Flow in the Valley of Ten Thousand Smokes, Alaska. Geology, 28, 835–838.

Whittaker, J.G. (1987) Modelling bed-load transport in steep mountain streams. Erosion and Sedimentation in the Pacific Rim (Proceedings of the Corvallis Symposium), IAHS, Publication 165, Vancouver, 319–332.

Whittaker, A.C., Attal, M. and Allen, P.A. (2010) Characterising the origin, nature and fate of sediment exported from catchments perturbed by active tectonics. Basin Res., 22, 809–828.

Whittaker, A.C., Duller, R.A., Springett, J., Smithells, R., Whitchurch, A.L. and Allen, P.A. (2011) Decoding downstream trends in stratigraphic grain-size as a function of tectonic subsidence and sediment supply. Bull. Geol. Soc. Am., 123, 1363–1382.

Wilcock, P.R. (1993) Critical shear stress of natural sediments. J. Hydraul. Eng., 19, 491–505.

Wilcock, P.R. (2001) Toward a practical method for estimating sediment-transport rates in gravel-bed rivers. Earth Surf. Proc. Land., 26, 1395–1408.

Wilcock, P.R. and McArdell, B.W. (1997) Partial transport of a sand/gravel sediment. Water Resour. Res., 33, 235–245.

Wohl, E.E. (1992) Bedrock benches and boulder bars: Floods in the Burdekin Gorge, Australia. Geol. Soc. Am. Bull., 104, 770–778.

Wolman, M.G. (1954) A method of sampling coarse river bed material. Am. Geophys. Union Trans., 35, 951–956.

Wolman, M.G. and Gerson, R. (1978) Relative scales of time and effectiveness of climate in watershed geomorphology. Earth Surf. Proc. Land., 3, 189–208.

Wolman, M.G. and Miller, J.P. (1960) Magnitude and frequency of forces in geomorphic processes. J. Geol., 68, 54–74.

Yanites, B.J., Tucker, G.E., Mueller, K.J., Chen, Y.G., Wilcox, T., Huang, S.Y. and Shi, K.W. (2010) Incision and channel morphology across active structures in the Peikang River, central Taiwan: implications for the importance of channel width. Bull. Geol. Soc. Am., 122, 1192–1208.

Figures

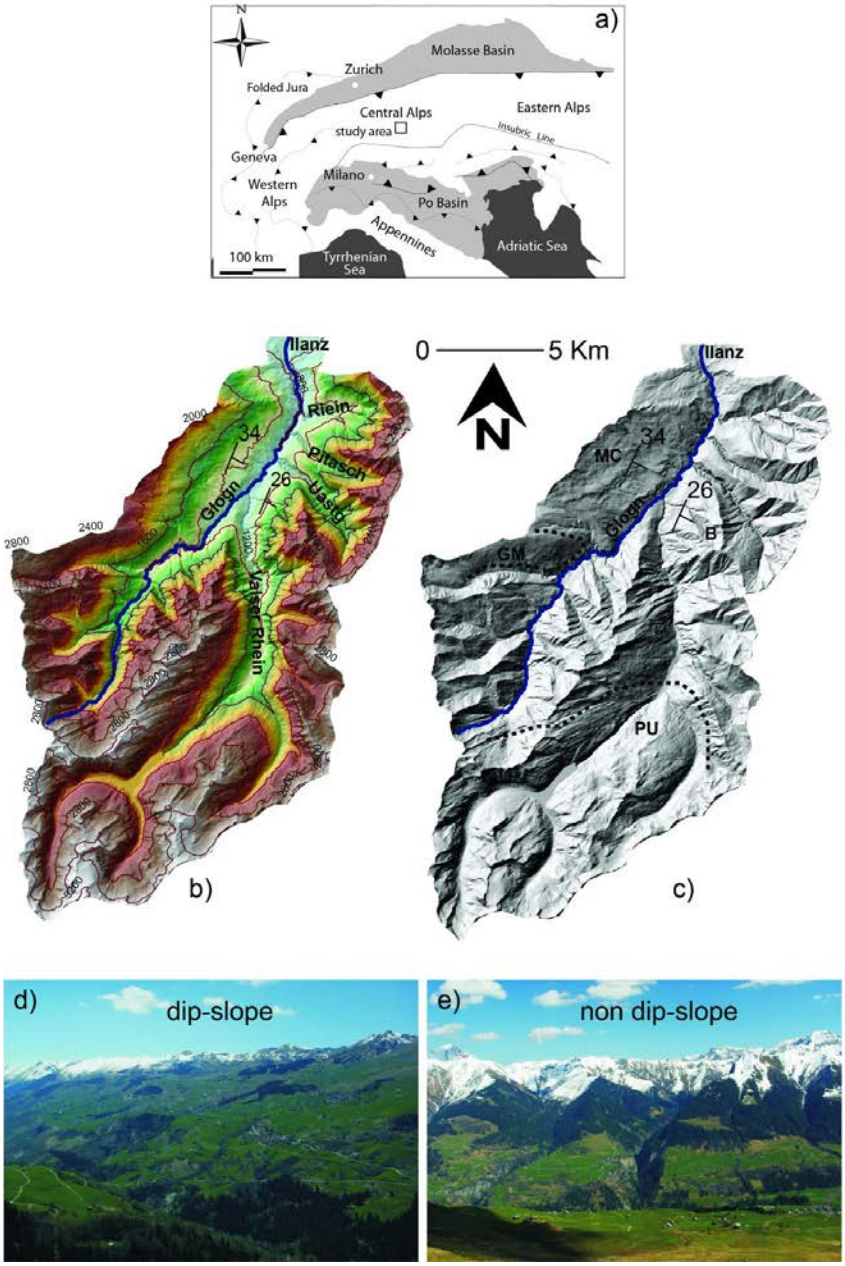

Fig. 1. Geomorphological and geological setting of the study area. **(A)** Geographic and tectonic location of the study area. **(B)** Geomorphic setting of the study area. **(C)** Geological setting of the study area and the surrounding geological units: 'MC' Mezosoic Cover on the western flank; 'B' Bündnerschiefer; 'GM' Gotthard Massif; and 'PU' Penninic Unit. **(D)** and **(E)** Contrasting hillside morphology in dip slope (western valley side) and non-dip slope (eastern valley side) situations, respectively; hillslopes are smooth and gently dipping in (D) whereas they are steep and deeply dissected in (E).

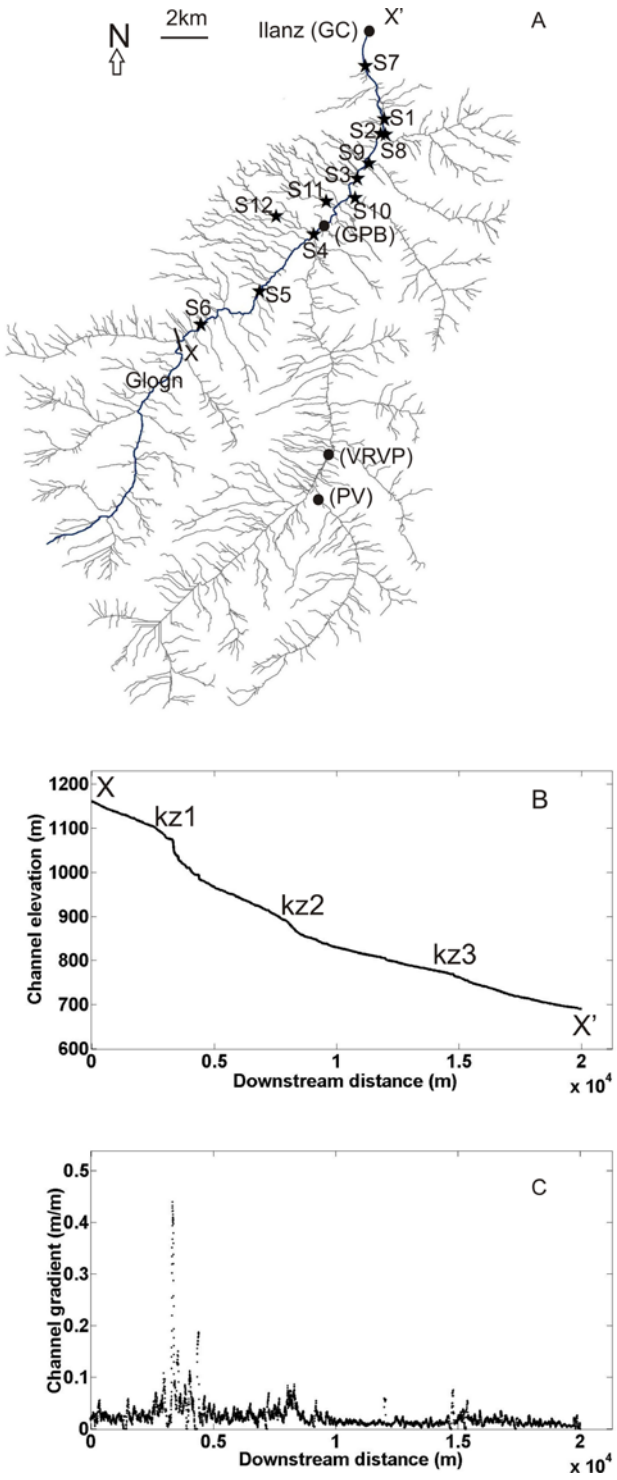

Fig. 2. (A) Hydrological map of the study area with sites where sediment grain-size distribution was measured in the field (stars). Circles represent the hydrological gauging stations. **(B)** and **(C)** Channel longitudinal profile and downstream variations in channel gradient, respectively. Channel gradients were extracted from a 2 m resolution digital elevation model (DEM) taking the average gradient over a constant vertical drop of 2 m. Note the presence of three knickzones ('kz') along the channel.

Fig. 3. Field measurement sites along the trunk channel. **(A)** Site (S6) is upstream of the major knickzone (kz1). **(B)** Site (S5) is downstream of the major knickzone. **(C)** Site (S4) is at the confluence with the Valser Rhein. **(D)** Site (S3) is a large boulder bar with angular particles. **(E)** Site (S2); note the large gravel bar and the exposure of bedrock on the side. **(F)** Site (S1); note that the coarse boulders are most likely to be supplied by the Val Riein River. **(G)** Site (S7) is a very large and well-imbricated boulder bar covering almost the entirety of the channel bed. (H) Photograph of site (S7) shows a boulder with the typical bedrock lithology of the region.

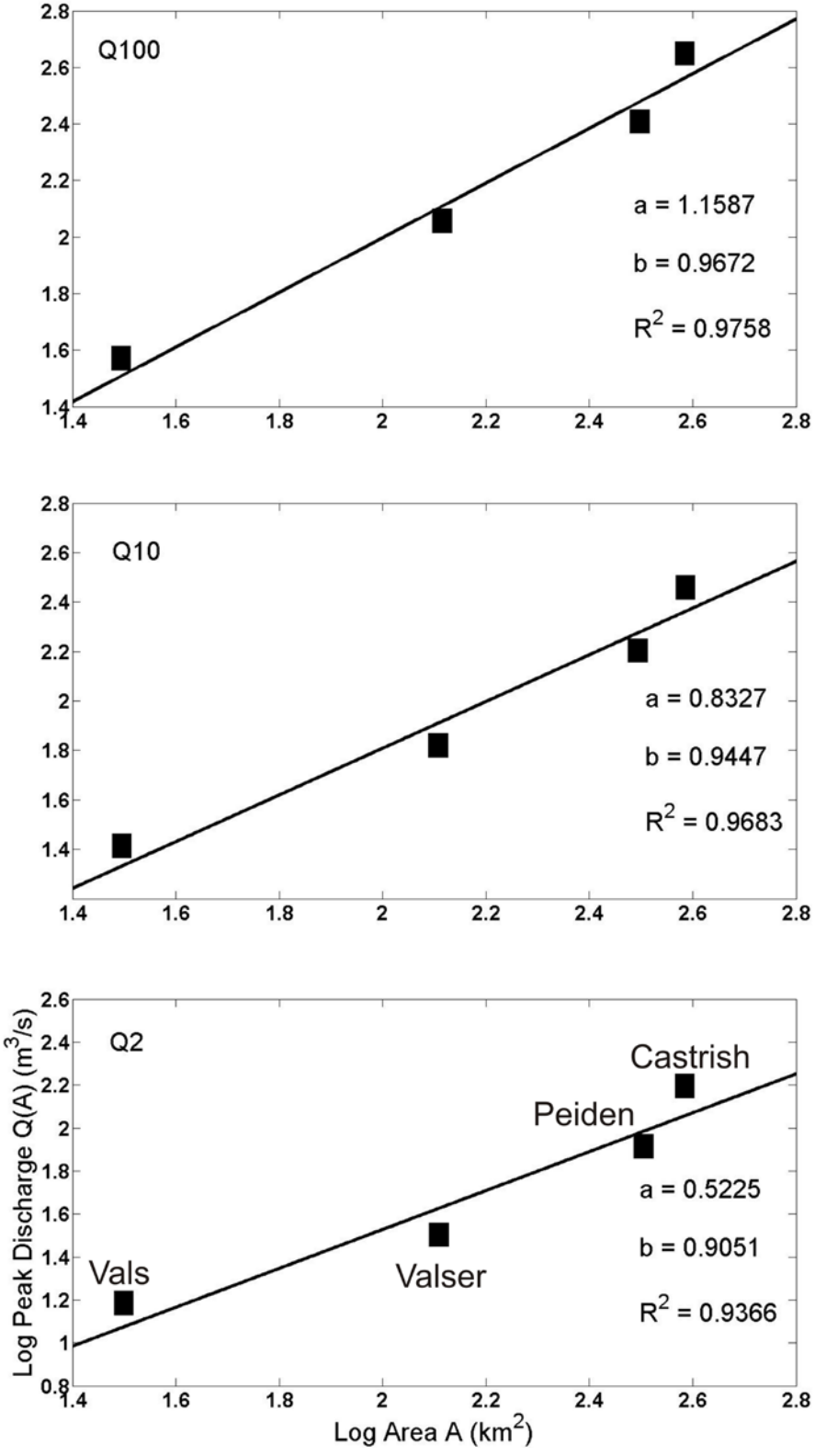

Fig. 4. Log-discharge (m^3/s) versus log-drainage area (km^2) for three events in the Val Lumnezia basin. The regression intercept and slope are $\log(a_T)$ and b_T in Eq. 1.

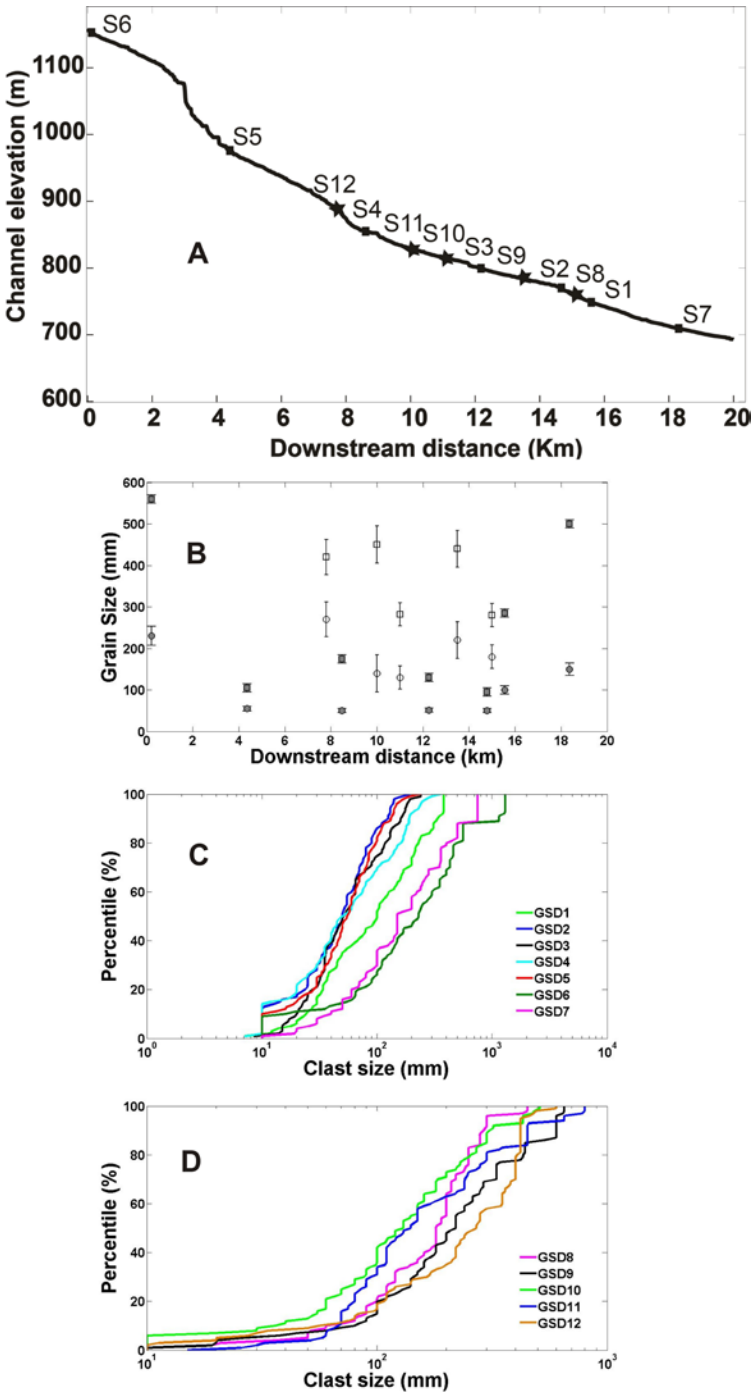

Fig. 5. (A) Channel longitudinal profile with all sites where grain sizes were measured in the Glogn trunk channel (squares) and in the tributaries on both sites (stars). Sites 11 and 12 are located on the western valley side, whereas sites 8, 9 and 10 are located in the tributary channels on the eastern valley side. **(B)** Error bars for *D84* (squares) and *D50* (circles) measured in the trunk stream (filled symbols) and in the tributaries (opened symbols). **(C)** and **(D)** Cumulative distribution curves of particle sizes measured in the trunk stream and the tributaries, respectively.

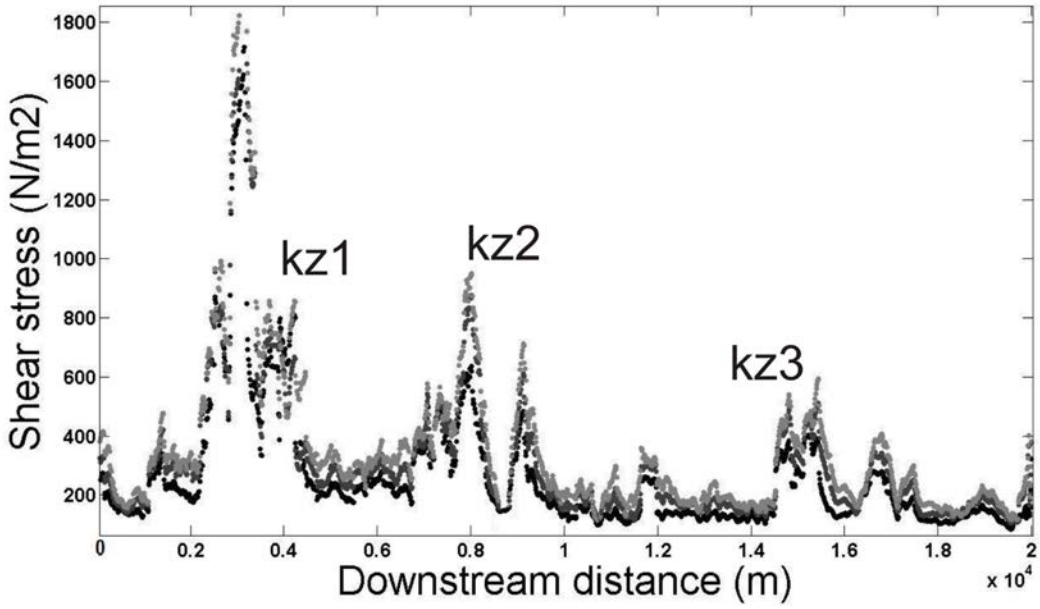

Fig. 6. Downstream variation in the boundary shear stress along the trunk stream for floods with return periods of two, 10 and 100 years in dark, grey and grey white, respectively. Note the systematic increase in shear stress along the entire stream with increasing flood magnitude. The peaks are located in the three knickzones (kz).

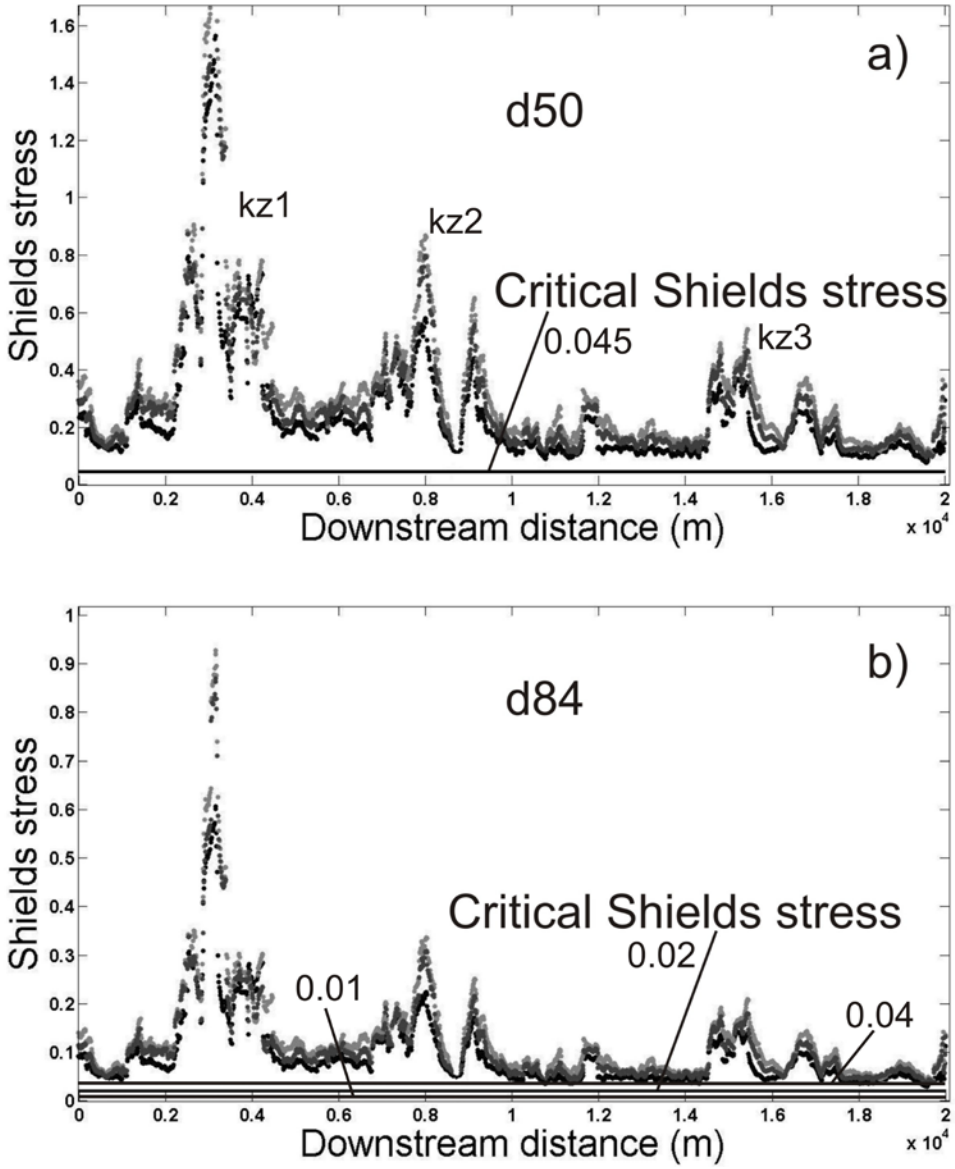

Fig. 7. (A) Shields stress curves showing the potential for entrainment of *D50* along the entire channel during two, 10 and 100 years floods in dark, grey and grey white, respectively. Note the systematic increase in shear stress over the knickzones leading to potential entrainment of *D50* during all flood events. The flat reaches show a high potential for entertainment of *D50* also for the two year flood. **(B)** Shields stress curves showing the potential for entrainment of *D84* during two, 10 and 100 year floods. Note the increase in the critical Shields stress, which is related to the decrease of the size of *D84* (see text for further explanation). Note also that the critical Shields stress was calculated considering the maximum (560 mm), minimum (100 mm) and mean values (270 mm) of *D84* for all sites, yielding the three critical values of 0.01, 0.02 and 0.04, respectively.

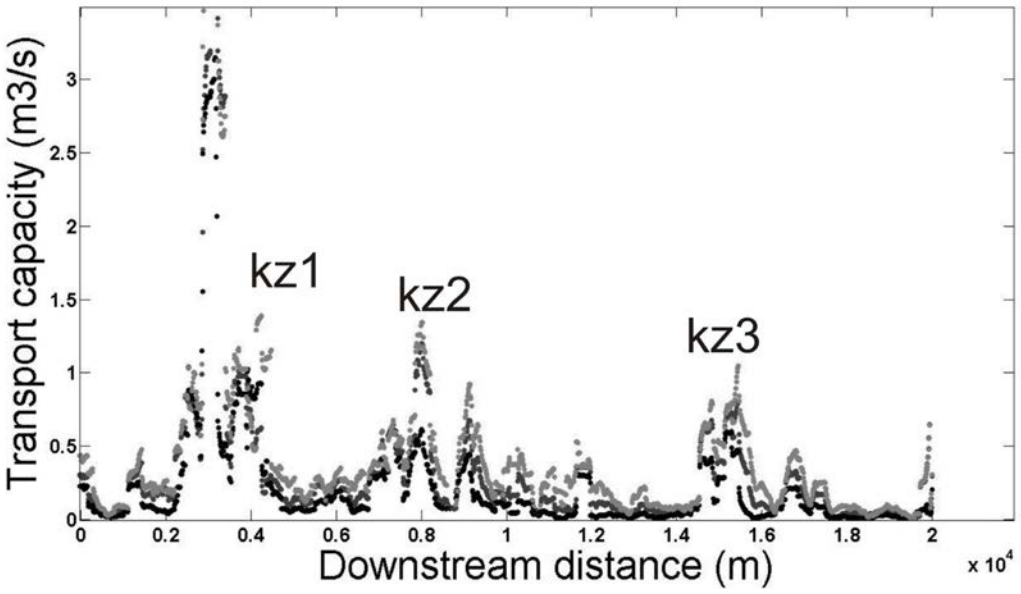

Fig. 8. Predicted sediment transport capacity for floods of two, 10 and 100 year return periods in dark, grey and grey white, respectively. Note that the knickzones have a high transport capacity for all floods (highest values); meanwhile the flat segments show relatively low transport capacity values even for the centennial floods.